

The Use of Mercury Intrusion Porosimetry or Helium Porosity to Predict the Moisture Transport Properties of Hardened Cement Paste

G. Hedenblad

Division of Building Materials, Lund Institute of Technology, Lund, Denmark

The moisture permeability of hardened cement paste is normally not a constant, because it depends on both the porosity and the relative humidity (RH) in the pores of the cement paste when RH exceeds approximately 60 to 70%. The measured results show a strong relationship between the porosity of the cement paste and the moisture permeability. ADVANCED CEMENT BASED MATERIALS 1997, 6, 123–129. © 1997 Elsevier Science Ltd.

KEY WORDS: Capillary porosity, Cement paste, Mercury intrusion porosity, Moisture permeability, Permeability, Porosity

Relating microstructure to the moisture transport properties of building materials is of great interest for predicting the performance of a material in a given environment. For instance, how does a change of the composition of a concrete influence the moisture state in a given structure? In the EU project "Characterisation of microstructure as a tool for prediction of moisture transfer in porous materials," seven different laboratories co-operated to study microstructure and macroscopic coefficients with different methods. One goal in the project was to develop both computer models and an empirical evaluation of the relation between the microstructure and the moisture transport properties. A network model was developed by Quenard et al. [1] at CSTB in France. This article is an attempt to find a simplified relation between the microstructure and the moisture transport properties of cement paste.

Experiments

Materials

Five different cement pastes were mixed at the Building Materials Laboratory, Technical University of Denmark

(LBM). The five mixes, with different water/cement ratios (w_0/C), were based on Ordinary Portland Cement (OPC) from Le Teil, France. Two of the mixes had additives, silica fume (SF) and slag (s). The five mixes were (1) OPC, $w_0/C = 0.35$; (2) OPC + 10% silica fume + 1.8% Lomar-D copolymer, $w_0/C = 0.2$; (3) OPC, $w_0/C = 0.45$; (4) OPC (30%) + s (70%), $w_0/(C + s) = 0.35$; and (5) OPC, $w_0/C = 0.6$. The s used was from England. Chemical analysis of OPC, SF and s are given in Hansen [2].

The cast samples have a cylindrical geometry with a length of ca 100 mm and a diameter of ca 23 mm. During the mixing and the casting, special care was taken to avoid nonhomogeneity. After casting, the samples were cured in lime water at constant temperature for at least 4 months before they were sent to the other laboratories involved in the project.

Measurement of the Porosity of the Materials

The porosity of the hardened cement pastes was measured with mercury intrusion porosimetry (MIP) at two laboratories, Fraunhofer-Institut für Bauphysik (IBP) in Holzkirchen, Germany, and Laboratoire Central des Ponts et Chaussées (LCPC) in Paris, France. At both institutions the MIP measurements were performed on predried specimens using a CARLO ERBA 2000 WS porosimeter [3,4]. The cumulative pore size distributions measured at IBP and LCPC were nearly the same [3]. According to Krus et al. [4] the lowest pore diameter that can be registered by this MIP equipment is approximately 0.4 nm.

The laboratory at IBP used a helium pycnometer to measure the true density of the materials. Small samples were dried at 105°C, with dry air. As they dried, the air inside the pores was replaced with helium and the amount of the inert gas was detected. Knowing the bulk density, the open porosity was then calculated.

Address correspondence to: Göran Hedenblad, Division of Building Materials, Lund Institute of Technology, Box 118, 221 00 Lund, Sweden.
Received March 21, 1997; Accepted August 8, 1997

TABLE 1. Measured porosities of the five different hardened cement pastes [4]

Cement Paste	Helium Porosity (vol.-%)	MIP Porosity (vol.-%)
$w_0/C = 0.35$	14	15
$w_0/C = 0.2 + 10\% \text{ SF}$	7.3	7.6
$w_0/C = 0.45$	22	24
$w_0/(C + s) = 0.35$	12	9
$w_0/C = 0.6$	31	29

The smallest pore measured by helium pycnometry is ca 0.22 nm [4].

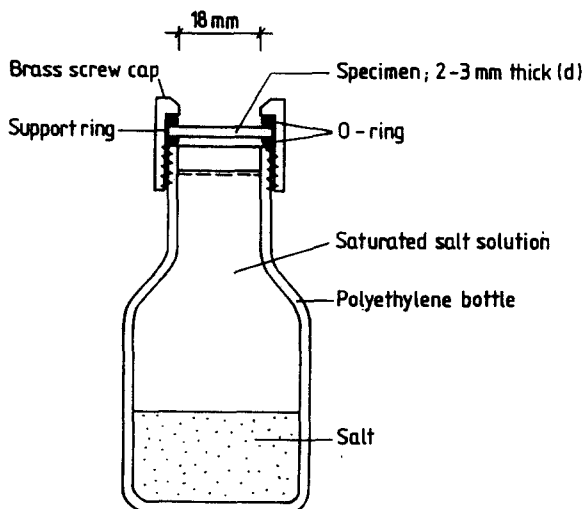
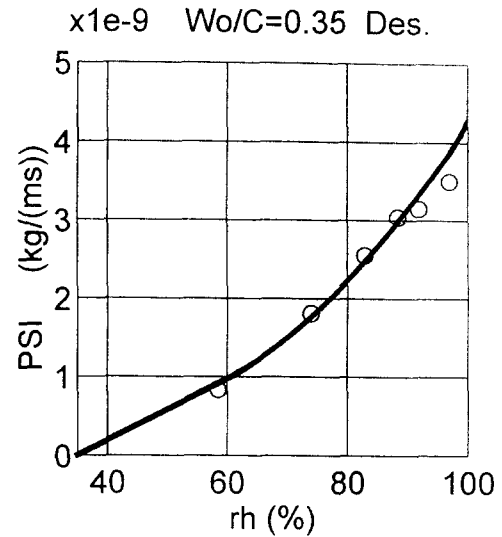
The porosities of the 5 hardened cement pastes determined with MIP and helium pycnometry are shown in Table 1 [4]. Table 1 shows that the porosities measured by the two different techniques are nearly the same for the same cement paste, which was also shown by March et al. [5] in 1983.

Measurement of the Moisture Transport Coefficients

For many materials, the moisture permeability (δ_v or δ_p) is not constant, but varies with the moisture content [or the relative humidity (RH)] in the material and with the temperature. The definition of δ_v is taken from the standard ISO 9346:1987, and in one dimension one has

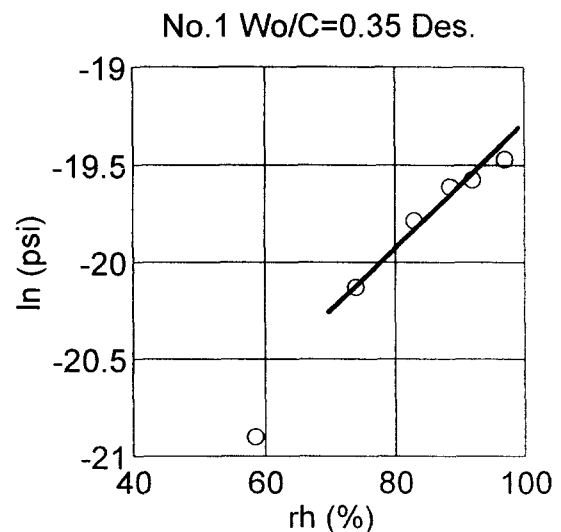
$$g = \delta_v \cdot \frac{\partial v}{\partial x} \quad (1)$$

where g is the density of moisture flow rate [$\text{kg}/(\text{m}^2 \cdot \text{s})$]; δ_v is the moisture permeability with regard to humidity by volume (m^2/s); and v is the humidity by

**FIGURE 1.** Moisture permeability cup.**FIGURE 2.** CP no. 1: the Ψ -potential as a function of RH.

volume in the pores of the material (kg/m^3). By using the cup method in a special way it is possible to measure the moisture permeability as a function of the RH. A cup is shown in Figure 1.

The RH outside the cup is ca 35%, and inside the cup it is approximately 60, 75, 82, 85, 90, 95, 98, or 100%. These RHs are achieved with saturated salt solutions (except 100%). The top of the cup (including the specimen) is removable, and the cup can be refilled with liquid. This means that the liquid surface in the cup can be nearly constant and close to the bottom of the sample. This is important for open materials. When the moisture flow rate from a cup has been constant for a period of time, the weight changes are measured as

**FIGURE 3.** CP no. 1: logarithm of the Ψ -potential as a function of RH.

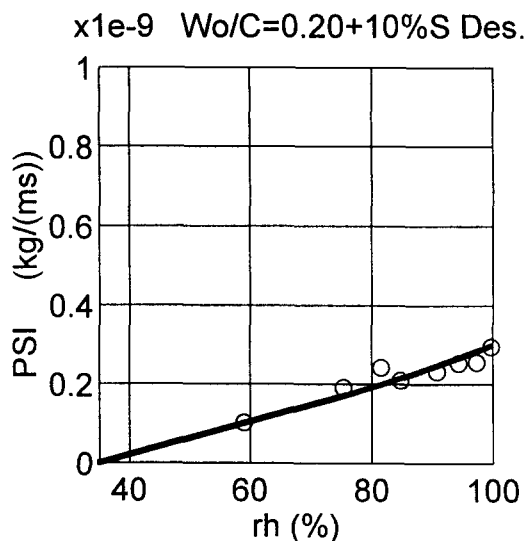


FIGURE 4. CP no. 2: the Ψ -potential as a function of RH.

functions of time. The moisture flow rate (g) multiplied by the thickness (d) of the sample is called the Kirchhoff potential (Ψ). The Kirchhoff potential is used in the Results section, but because the thicknesses of the samples are nearly the same, Ψ is, in principle, the moisture flow rate.

Results

Moisture Transport Coefficients

Figures 2 through 11 illustrate the Kirchhoff potential as a function of RH for the five studied cement pastes under desorption (Des). The slope of the Ψ -RH curves

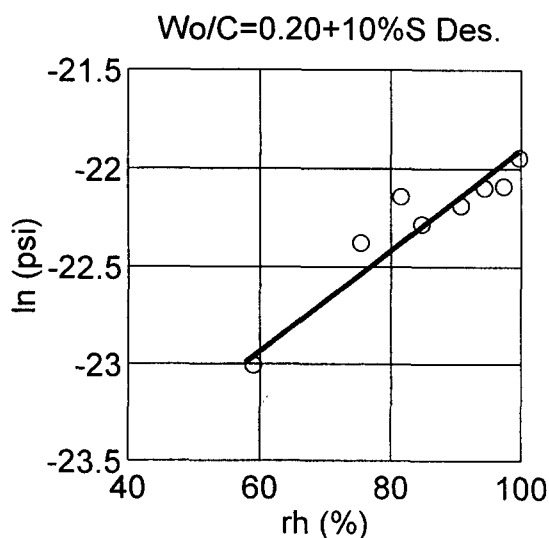


FIGURE 5. CP no. 2: logarithm of the Ψ -potential as a function of RH.

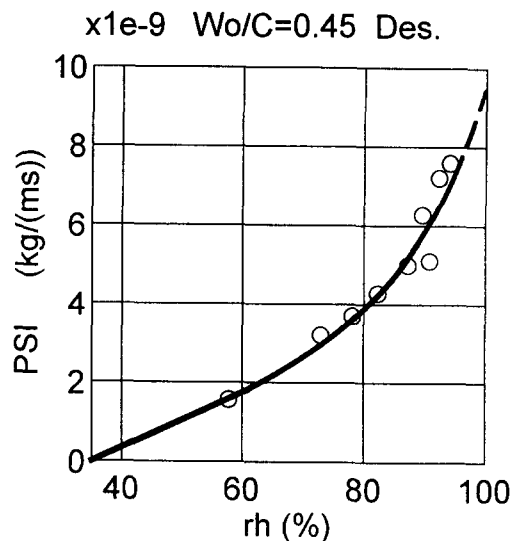


FIGURE 6. CP no. 3: the Ψ -potential as a function of RH.

in these figures is, in principle, the moisture permeability at each RH. Therefore, if the Ψ -RH relation is a straight line, the moisture permeability is constant.

In Figures 2 through 11, the natural logarithms of the Ψ -potential are also shown as functions of RH. This is done because at higher RH the Ψ -RH relationship becomes, in this scale, a nearly straight line. The highest measured result is not at 100% RH, because there is a moisture resistance in the air gap between the specimen and the liquid. This moisture resistance lowers the RH at the bottom of the sample to a value lower than the RH of the salt solution. The straight line in the figures is extrapolated to 100% RH. In this way one can get a probable value of Ψ at 100% RH.

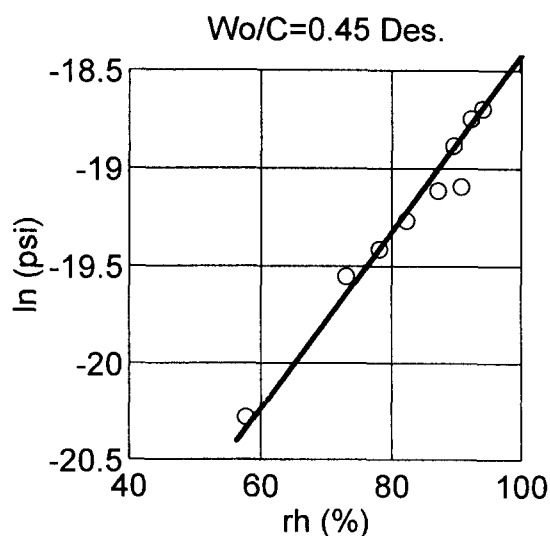
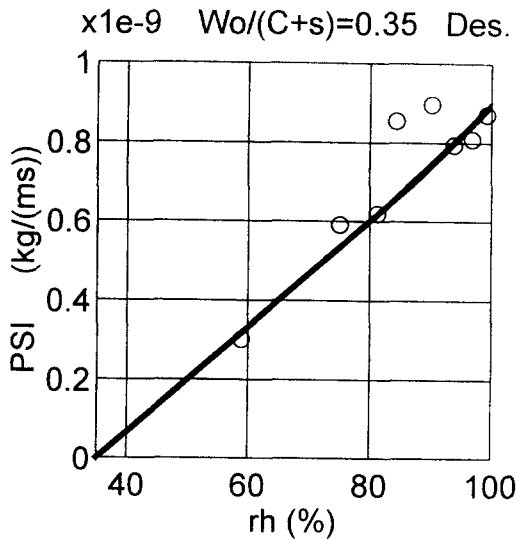
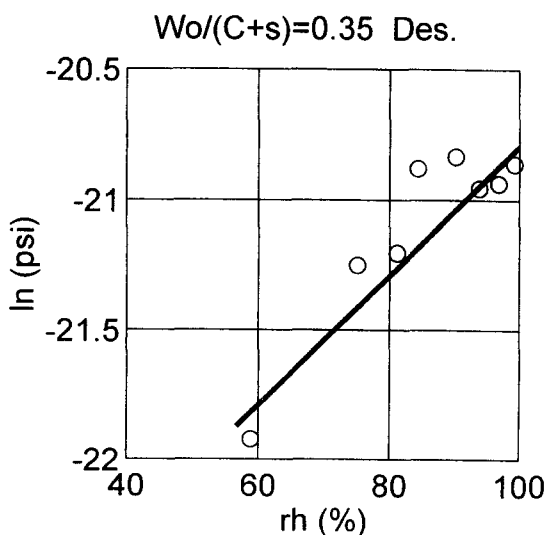
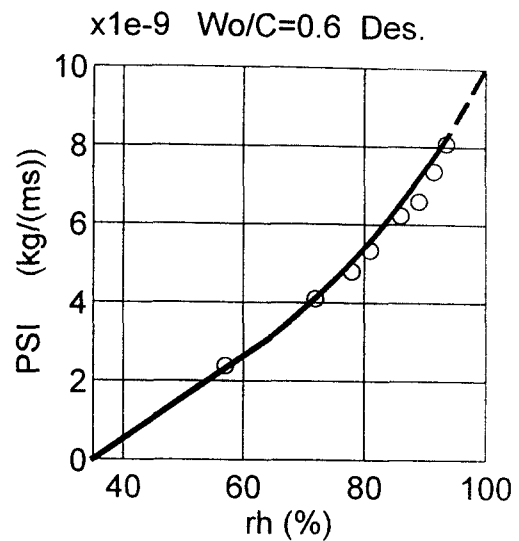


FIGURE 7. CP no. 3: logarithm of the Ψ -potential as a function of RH.

FIGURE 8. CP no. 4: the Ψ -potential as a function of RH.

In the figures for the Ψ -RH relationship, there is a nearly straight line at lower RH, between 35% up to approximately 60 to 70% RH. This nearly linear relationship at lower RH has also been measured in an another study, with a different measurement technique [8]. In Figures 2 through 11, only results for specimens under desorption are shown. There are also results for specimens under absorption, but they are not reported here. The moisture permeability can also be calculated by

$$\delta_v = \frac{\partial \Psi}{\partial v} = \frac{\partial \Psi}{\partial rh \cdot v_s} \quad (2)$$

FIGURE 9. CP no. 4: logarithm of the Ψ -potential as a function of RH.FIGURE 10. CP no. 5: the Ψ -potential as a function of RH.

where v_s is v at saturation (RH = 100%). In this way the moisture permeability is determined at low RH and at 100% RH. The results are shown in Table 2.

Moisture Permeability versus Measured Porosity

The results of plotting the moisture permeabilities at low RH (Table 2) against the porosity are shown in Figure 12. Here the mean value between MIP and helium porosity is used. Figure 12 shows that there is a nearly linear relationship between δ_v at low RH and the porosity. The correlation coefficients for the linear re-

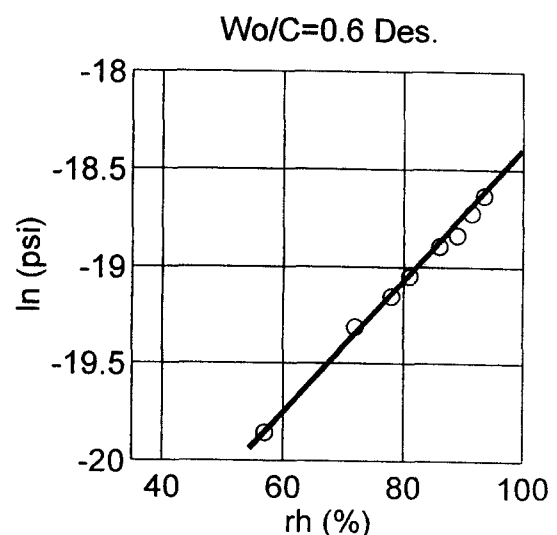
FIGURE 11. CP no. 5: logarithm of the Ψ -potential as a function of RH.

TABLE 2. Moisture permeability (m^2/s) at low RH (from 35% up to approximately 60 to 70% RH) and at 100% RH

Cement Paste	Desorption		Absorption	
	Low RH	100% RH	Low RH	100% RH
$w_0/C = 0.35$	$0.22 \cdot 10^{-6}$	$0.84 \cdot 10^{-6}$	$0.13 \cdot 10^{-6}$	$1.05 \cdot 10^{-6}$
$w_0/C = 0.20 + \text{SF}$	$0.024 \cdot 10^{-6}$	$0.034 \cdot 10^{-6}$	$0.018 \cdot 10^{-6}$	$0.038 \cdot 10^{-6}$
$w_0/C = 0.45$	$0.41 \cdot 10^{-6}$	$1.75 \cdot 10^{-6}$	$0.25 \cdot 10^{-6}$	$1.4 \cdot 10^{-6}$
$w_0/(C + s) = 0.35$	$0.077 \cdot 10^{-6}$	$0.15 \cdot 10^{-6}$	$0.017 \cdot 10^{-6}$	$0.17 \cdot 10^{-6}$
$w_0/C = 0.60$	$0.61 \cdot 10^{-6}$	$2.2 \cdot 10^{-6}$	$0.52 \cdot 10^{-6}$	$2.1 \cdot 10^{-6}$

gressions in Figure 12 are 0.99 for desorption and 0.97 for absorption.

The results of plotting the moisture permeabilities at 100% RH (Table 2) against the porosity squared are shown in Figure 13. Although δ_v at 100% RH is calculated from extrapolated Ψ values, there seems to be a nearly linear correlation between δ_v and the squared porosity. The correlation coefficient for all results in Figure 13 is 0.96. Gilliland et al. [6] and Flood et al. [7] have given equations for moisture transport that, in principle, include the squared porosity [8].

With the empirical relationships given in Figures 12 and 13, it is possible to predict figures of δ_v at low RH and at 100% RH when the MIP or the helium porosity is known. These porosities are much less time-consuming to determine than the moisture permeability.

To estimate the moisture permeability between approximately 60% RH and 100% RH, different equations can be used, but here the following is studied

$$\delta_v = \delta_v^{60\%} + (\delta_v^{100\%} - \delta_v^{60\%}) \left(\frac{rh - 60}{40} \right)^3 \quad (3)$$

Other equations can probably provide better agreement with the measured moisture permeabilities, but eq 3 is simple to use. The estimated moisture permeabilities determined using the above equation together with Figures 12 and 13 are compared in Figures 14 through

17, with the δ_v derived directly from the slope of the Ψ -RH curves for some of the hardened cement pastes. The results for CP no. 2 are only shown in Table 2, as δ_v at low RH is nearly the same as at 100% RH.

Based on the results from CP no. 1, no. 3, and no. 5, the relationship between δ_v and w_0/C (for OPC) can be established. The corresponding model may provide engineers with a useful tool to simply predict moisture permeability of a material by knowing w_0/C ratio, the degree of hydration (see Figure 19), and RH. In Figures 14 through 17 it is important to realize that all the Y axes have different scales. This is done because the moisture permeabilities are so different for the different cement pastes.

The Use of MIP Porosity to Predict all Water Transport Processes

It is likely that when knowing the MIP or helium porosity for a hardened cement paste it is possible to predict the moisture permeability, the water permeability, and to some extent, the capillary uptake of water. Christensen et al. [9] have shown a relationship between, in principle, the MIP and the water permeability. Freitas et al. [10] published results for the capillary suction of hardened cement pastes. The water uptake by capillary suction is normally given by the following two equations

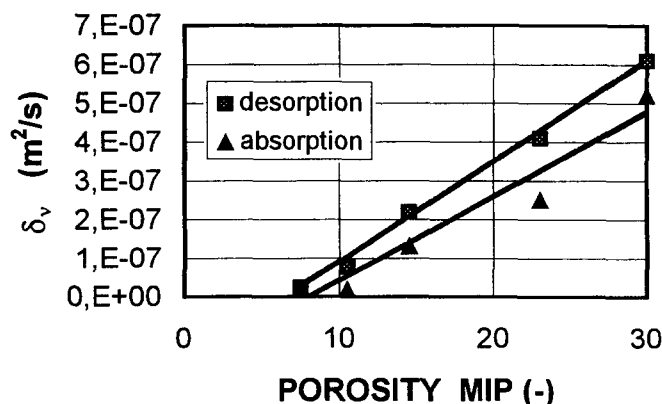


FIGURE 12. δ_v at low RH as a function of the MIP porosity.

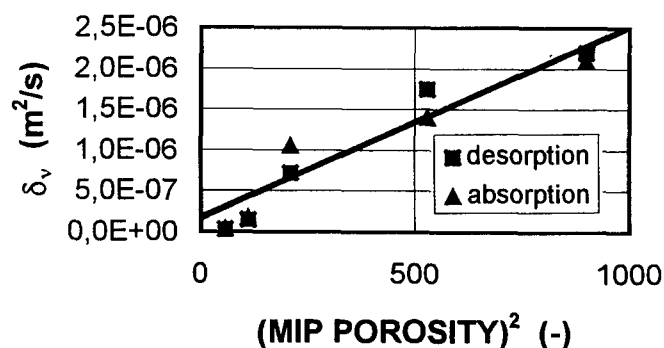


FIGURE 13. δ_v at 100% RH as a function of the squared MIP porosity.

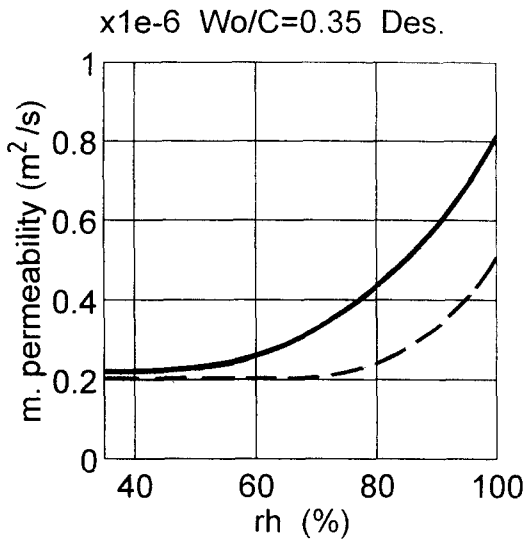


FIGURE 14. CP no. 1: the estimated and directly calculated δ_v as functions of RH; solid line = measured, broken line = calculated.

$$m_s = A \cdot \sqrt{t} \quad (4)$$

and

$$x = B \cdot \sqrt{t} \quad (5)$$

where m_s is the mass divided by area of sorbed water from a water surface (kg/m^2); t is time (s); A is the water sorption coefficient [$\text{kg}/(\text{m}^2 \cdot \text{s}^{1/2})$]; x is the penetration depth of water front during sorption from a water surface (m); and, B is the water penetration coefficient ($\text{m}/\text{s}^{1/2}$).

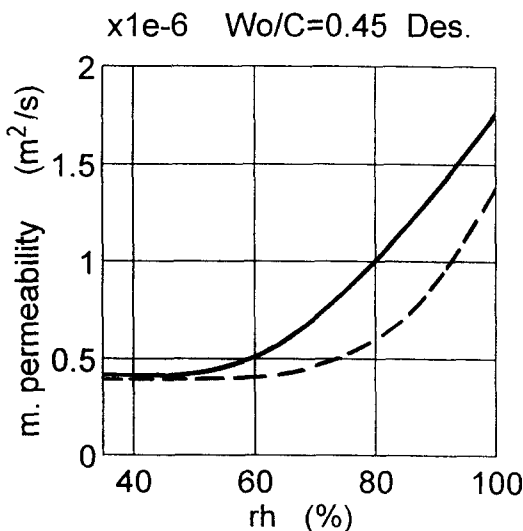


FIGURE 15. CP no. 3: the estimated and directly calculated δ_v as functions of RH; solid line = measured, broken line = calculated.

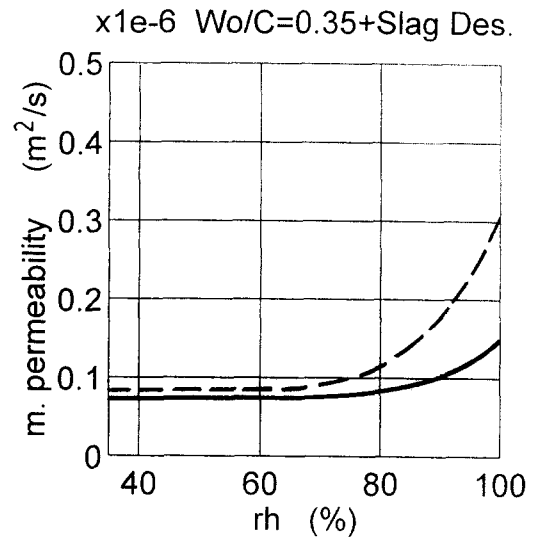


FIGURE 16. CP no. 4: the estimated and directly calculated δ_v as functions of RH; solid line = measured, broken line = calculated.

Figure 18 is a graphic representation of the results of de Freitas et al. [10]. However, it should be emphasized that the above relationships do not always describe the whole process of capillary uptake in hardened cement pastes. For low MIP porosity, the equations only describe the first part of the capillary uptake.

An Empirical Relation Between the MIP and the Capillary Porosity

Fagerlund [11] has hypothesized that all moisture and water transport coefficients depend on the capillary

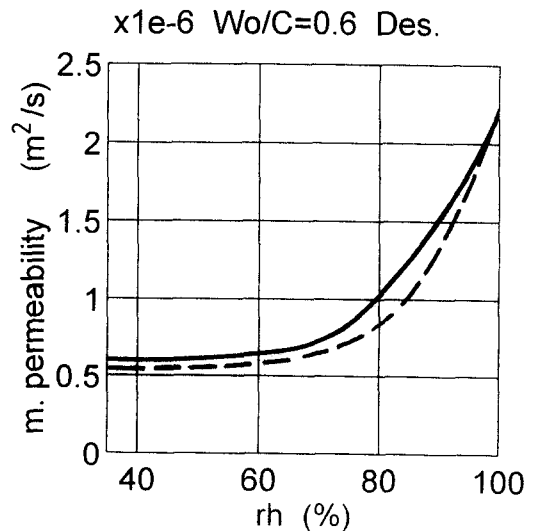


FIGURE 17. CP no. 5: the estimated and directly calculated δ_v as functions of RH; solid line = measured, broken line = calculated.

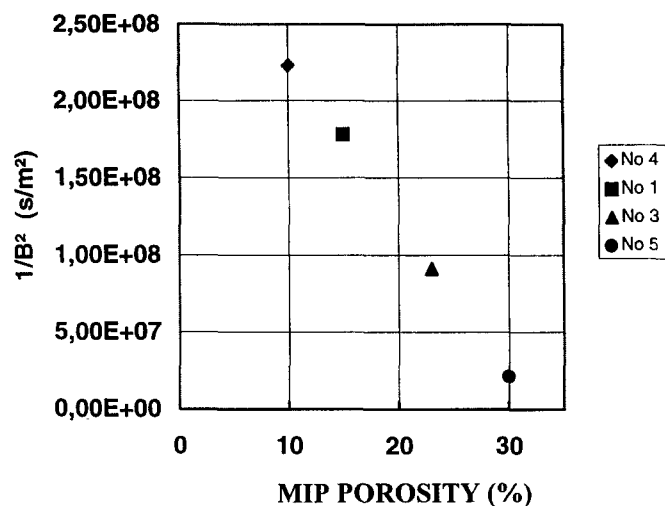


FIGURE 18. The capillary coefficient B as a function of the MIP porosity.

porosity. Halamickova [12] has measured both the degree of hydration (α) and the MIP pore size distribution for cement pastes with w_0/C of 0.4 and 0.5. In the project reported here, α was not measured, but α can be estimated from the measured porosities. In Figure 19, the capillary porosity is shown as a function of the MIP porosity.

In the results of Halamickova, the MIP porosities have been read at the same pore size as in this project. Figure 19 shows that there seems to be a nearly linear relationship between the MIP porosity and the capillary porosity. If this is so, it may be possible to predict all the moisture and water transport coefficients for an OPC paste just by knowing w_0/C and α . Bentz [13] has shown that α can be measured with quite different techniques.

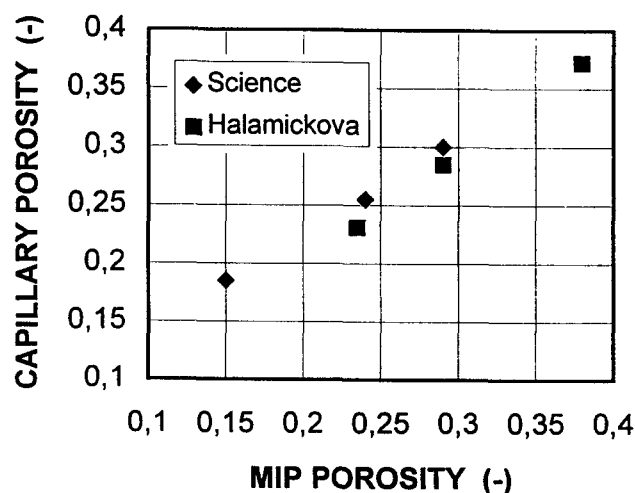


FIGURE 19. Capillary porosity as a function of the MIP porosity.

Conclusions

It seems possible to predict moisture permeability with the aid of the given empirical relationships. Of course, these must be verified with independent tests. However, when judging the model, the differences in δ_v , when measured at different laboratories, have also to be taken into consideration. The results of a round-robin test showed that there were large differences between laboratories in the measured δ_v [14].

Acknowledgments

The project was supported by the Commission of the European Communities, the Directorate General XII for Science, Research and Development. The Swedish Council for Building Research has supported the work done at our laboratory. My sincerest thanks to Dr. Wojciech Roszak, who with extreme care did the experimental work on the determination of the moisture permeability as a function of the relative humidity.

References

1. Quenard, D.; Daian, J.; Xu, K. Multiscale models: A tool to describe the porosity of cement-based materials and to predict their transport properties. Workshop NATO/RILEM—Saint Rémy les Chevreuse, July 1994.
2. Kielsgaard Hansen, K. In Characterisation of microstructure as a tool for prediction of moisture transfer in porous media. Annual report 1 of the Science Project, CT91-0737 to the Commission of the European Communities. Directorate General XII for Science, Research & Development, 1993.
3. Kielsgaard Hansen, K.; Baroghel-Bouny, V.; Künz, H.M. In *Proceedings of the 4th Symposium on Building Physics in the Nordic Countries*; Espoo, Finland, 1996, pp 755–762.
4. Krus, M.; Künz, H.M.; Kielsgaard Hansen, K. *Materials and Structures*, 1997, 30, 394–398.
5. Marsh, B.K.; Day, R.L.; Bonner, D.G.; Illston, J.M. *Proceedings, Principles and Applications of Pore Structural Characterisation*, Milan, Italy, 1983.
6. Gilliland, E.; Baddour, R.; Russel, J.L. *American Institute of Chemical Eng.* 1958, 4, 90–96.
7. Flood, E.A.; Tomlinson, R.H.; Leger, A.E. *Canadian Journal of Chemistry* 1952, 30, 348–410.
8. Hedenblad, G. Division of Building Materials, Lund Institute of Technology, Sweden, Report TVBM-1014, 1993.
9. Christensen, B.C.; Mason, T.O.; Jennings, H.M. *Cement and Concrete Research*, 1996, 26(9), 1225–1334.
10. de Freitas, V.P.; Krus, M.; Künz, H.; Quenard, D. *Proceedings of the International Symposium on Moisture Problems in Building Walls*, Departamento de Engenharia Civil-Faculdade de Engenharia Universidade do Porto, Portugal, September 1995, 445–460.
11. Fagerlund, G. Division of Building Materials, Lund Institute of Technology, personal communication, 1994.
12. Halamickova, P. Master's Thesis. Department of Civil Engineering, University of Toronto, Canada, 1993.
13. Bentz, D.P. Building and Fire Research Laboratory, National Institute of Standards and Technology, Gaithersburg, MD, USA. Report NISTIR 5756.
14. Galbraith, G.H. Commission of the European Communities, bcr information, Report EUR 14349 EN, Brussels, 1993.